

Design of Superhydrophobic Paper/Cellulose Surfaces *via* Plasma Enhanced Etching and Deposition

Balamurali Balu, Jong Suk Kim, Victor Breedveld and Dennis W. Hess*

School of Chemical and Biomolecular Engineering, Georgia Institute of Technology,
311 Ferst Drive, Atlanta, GA 30332-0100, USA

Abstract

Superhydrophobicity has been achieved on different paper surfaces *via* plasma enhanced etching and film deposition. The effects of fiber types and paper making parameters on the superhydrophobic behavior were studied. Achievement of superhydrophobic behavior depends on the formation of nano-scale features on the paper fibers established by selective etching of the amorphous domains in cellulose. Despite different fiber types and paper making processes, superhydrophobicity can be attained provided that plasma etching can occur on the fiber surface to create nano-scale features. Plasma processing conditions that allow the design of superhydrophobic paper or cellulose surfaces with specific adhesion properties are described. The significance of water drop volume on contact angle measurements and thus on characterization and analysis of superhydrophobic behavior of heterogeneous, porous paper substrates is discussed as well.

Keywords

Superhydrophobic, paper, cellulose, plasma, fibers, contact line

1. Introduction

Cellulose is an inexpensive biopolymer which is abundantly present in nature. Nevertheless, its inherent hydrophilic nature restricts direct use in a number of industrial applications such as printing, packaging and construction [1]. Hence, the hydrophilic fibers are often treated to make them hydrophobic *via* a process commonly referred to as “sizing” [2, 3]. For more than two hundred years, rosin (resin obtained from pine trees) based internal sizing agents have been added to pulp slurries to yield hydrophobic paper surfaces [3]. In recent decades, there have been significant developments in this field through advances in synthetic and polymer-based sizing agents [1, 2, 4–6]. An alternative approach for the internal sizing is external sizing where only the surface is coated with the sizing chemicals. Until recently, these methods (both external and internal) had generated hydrophobic

* To whom correspondence should be addressed. Tel.: (404) 894-5922; Fax: (404) 894-2866; e-mail: dennis.hess@chbe.gatech.edu

surfaces [7–10], but were not able to impart superhydrophobic (advancing contact angle (CA) $> 150^\circ$) characteristics to surfaces that are necessary to display extreme water repellency.

Superhydrophobicity can be achieved only by a unique combination of low surface energy and surface roughness. We recently reported the fabrication of superhydrophobic paper surfaces (advancing $CA \sim 166.7^\circ \pm 0.9^\circ$) using an external sizing method — surface modification *via* plasma processing [11]. Various other methods for the fabrication of superhydrophobic paper surfaces have also been reported recently [12–14]. However, these methods used a solvent based approach in at least one of the steps of fabrication. On the other hand, the plasma processing method that we have demonstrated is a vapor phase, solvent free, external sizing method. Moreover, the films formed using plasma deposition are mechanically robust because they are covalently bonded to the fibers. Indeed, adhesion between the coating and fibers is stronger than the adhesion between the fibers [11]. It was shown that superhydrophobic behavior on the paper or cellulose substrates resulted from the combination of a low surface energy fluorocarbon film deposited by plasma polymerization over cellulose fibers and roughness of these fibers on two separate length scales, i.e. on the nano- and micro-scale. While paper substrates have inherent micro-scale roughness as a result of the highly cross-linked web of cellulosic fibers, the nano-scale roughness was created by uncovering the crystalline domains on the cellulose fibers *via* oxygen plasma etching [11].

For superhydrophobic surfaces, the advancing contact angle (CA) defines the shape of a static drop, while the contact angle hysteresis (difference between the advancing and receding CA) defines the strength of adhesion of the drop. Hence, a superhydrophobic surface may yield different levels of adhesion for water drops (low water repellency to extreme water repellency) depending on the CA hysteresis values [15–21]. Clearly, an understanding of this fundamental aspect of superhydrophobicity is critical because it is related directly to the dynamics of water drops in contact with such substrates. Superhydrophobicity can be classified into two categories depending on the CA hysteresis values [11, 22]: (1) “roll-off” superhydrophobicity (advancing $CA > 150^\circ$, hysteresis $< 10^\circ$) and (2) “sticky” superhydrophobicity (advancing $CA > 150^\circ$, hysteresis $> 10^\circ$). As the names suggest, even for superhydrophobic surfaces, water drops can either roll off or stick to the substrate, depending on the CA hysteresis.

We have reported the fabrication of both “roll-off” and “sticky” superhydrophobic paper surfaces using plasma etching and deposition [11]. Recently, we described a methodology to tune the hysteresis (adhesion) between the two extreme behaviors and control the wetting mechanisms responsible for these behaviors [22]. The tunability in hysteresis was obtained by controlled formation of nano-scale features *via* selective plasma etching of the cellulose fiber surfaces. During paper manufacturing, the choice of fiber source and process conditions are chosen to meet the desired, application-specific properties. Based on our previous work, it is reasonable to expect that different types of paper, with different fiber sources and fiber treatments,

might display significant differences in micro-scale roughness (defined by the fiber web structure) and in the evolution of nano-scale roughness due to etching. Both of these factors are critical in determining their superhydrophobic behavior. In this contribution, we, therefore, investigate the impact of variations in fiber type and paper making process on the superhydrophobic properties of paper surfaces. The experiments also provide insight into the appropriate window of plasma processing conditions that enable design and fabrication of superhydrophobic paper surfaces for different applications. Finally, we discuss the effect of water drop size on contact angle and contact line geometry as observed in superhydrophobicity measurements on heterogeneous porous substrates such as paper.

2. Experimental

2.1. Paper Substrates

Five types of paper substrates were used for superhydrophobicity studies as described in Table 1. Handsheets (H, S, HS) were fabricated following the TAPPI method T205 sp-02 with southern hardwood kraft (Alabama River Pulp Co., Perdue Hill, AL) and/or southern softwood kraft (International Paper Co., Riegelwood, NC). Both of the fiber types (hardwood and softwood) were refined to the same level for a freeness value of ~ 500 prior to the paper forming process. Commercial copy paper substrates, “Premium white copy paper”, were obtained from local Office Depot. Commercial paper towels, SCOTT[®] High Capacity Hard Roll Towels (product code 01000) were manufactured by Kimberly-Clark.

2.2. Plasma Etching/Deposition

A 6-inch parallel plate rf (13.56 MHz) plasma reactor was used for plasma etching and deposition sequences; substrates were heated to 110°C. Details of the reactor configuration and operational procedures for the treatment of paper substrates can be found elsewhere [11]. Experimental conditions for oxygen etching and fluorocarbon (pentafluoroethane (PFE)) film deposition are listed in Table 2.

Table 1.
Paper substrates used for superhydrophobicity studies

Substrate designation	Description
H	Handsheet (100% hardwood fibers)
S	Handsheet (100% softwood fibers)
HS	Handsheet (50% hardwood–50% softwood)
CP	Copy paper
PT	Paper towel

Table 2.
Plasma reactor parameters for etching and deposition steps

Parameters	Etching	Deposition
Gas	Oxygen	Pentafluoroethane (PFE) and Argon (carrier gas)
Flow rate	75 sccm	20 sccm (PFE) and 75 sccm (Argon)
Pressure	0.55 Torr	1 Torr
Power	10 W	120 W
Treatment time	0–60 min	2 min

2.3. SEM Investigation

SEM micrographs were obtained using a LEO scanning electron microscope (model 1530) at an acceleration voltage of 5 kV or 10 kV depending on the damage induced by the electron beam on the paper surfaces. Prior to SEM studies, paper substrates were sputter coated (EMS 350; Electron Microscopy Sciences, Hatfield, PA) with a thin film of gold (~ 15 nm).

2.4. Water Contact Angle Measurements

For standard contact angle measurements, a 4 μ l water drop was used. Advancing and receding contact angles were measured by moving the substrate left to right with respect to the drop, following the methodology discussed by Gaudin *et al.* [23]. This method yields improved statistically averaged CA values relative to measuring CAs at individual locations independently, since a larger area of the substrate is scanned during measurement. However, for sticky substrates with receding CA less than 10° , this method could not be used because the drop breaks before the receding CA is attained; this limitation has been discussed in detail [23]. Our previous work [11] reported the receding CA observed during drop breakup which is not the true receding CA. To overcome this limitation inherent in Gaudin's method, we used the standard "volume decrement" method for sticky superhydrophobic substrates for which drop breakup was observed. Further details regarding the above contact angle measurement methods can be found elsewhere [22]. For our sticky superhydrophobic substrates, measurement of the advancing CA is also complicated. Interaction of the water drop with a "sticky" superhydrophobic paper surface is described by the Wenzel regime on a micrometer scale. The Wenzel regime is characterized by a very high hysteresis and therefore many closely placed metastable states [24]. This means that a range of advancing contact angles are possible depending on the force used to press the drop against the substrate. Since no quantitative measure of force was possible with the goniometer used, a slight variability in the advancing CA values was observed in the current studies relative to the CA values published previously [11]. For example, the advancing CA of sticky superhydrophobic HS reported in our Langmuir article [11] and this manuscript are $140^\circ \pm 1.7^\circ$ and $159.4^\circ \pm 7.7^\circ$, respectively.

2.5. Microscopic Imaging of the Contact Line

Drops with appropriate volumes were dispensed onto sticky superhydrophobic paper (HS) surfaces that had been attached to microscopic slides. The existence of a superhydrophobic contact angle made it impossible to obtain a clear microscopic image of three-phase contact lines due to the lensing effect of the drops. Hence, the water drops were allowed to evaporate until a hydrophilic contact angle was observed and the contact line was then imaged with a Leica microscope (DM4500 B) using a 10× objective.

3. Results and Discussion

3.1. Effects of Paper Making Parameters on Achievement of Superhydrophobicity

As discussed in the Introduction, the superhydrophobicity imparted to paper substrates results from the combination of a low surface energy film and two-scale roughness (nano-scale and micro-scale). The nano-scale roughness originates from the protrusion of crystalline domains on fiber surfaces after removal of the surrounding amorphous domains *via* selective plasma etching [11, 22]. On the other hand, the micro-scale roughness is determined by the topography of the paper fibers, in particular the fiber size and mesh size of the cellulose web. In this study we explore two key paper making parameters that may affect the micro- and nano-scale roughness and thus the resulting superhydrophobicity of paper substrates: (1) fiber source and (2) paper making technology.

3.1.1. Effects of Fiber Type

Cellulose paper is typically produced from hardwood fibers, softwood fibers, or a combination of the two. This classification of cellulose fibers is based on the trees from which they are obtained: hardwood fibers come from angiosperm trees (e.g., American yew, Common juniper, Douglas fir), and softwood fibers originate from gymnosperm trees (e.g., wild plum, peach, pear) [25, 26]. Both fiber types have approximately the same chemical composition: cellulose (40–50%), hemicellulose (25–35%) and lignin (20–35%), but there is a significant difference in physical dimensions [25]. Softwood fibers are usually larger than hardwood fibers roughly by a factor of two as shown in Table 3. Considering these facts, we expect that: (1) different cellulose fiber types would show differences with regards to the evolution of nano-scale roughness during etching (exposure of crystalline domains) and (2) the different fiber sizes will impact differently the micro-scale roughness of the paper

Table 3.
Typical dimensions of hardwood and softwood fibers [25]

Fiber type	Fiber length, mm	Fiber width, μm
Hardwood	1.0–1.5	16–22
Softwood	3.0–3.7	27–38

surfaces. We have shown previously that both length scales contribute to superhydrophobicity [11]. In order to investigate the role of fiber type in more detail, we fabricated handsheets from three different combinations of hardwood and softwood: 100% hardwood (H), 100% softwood (S) and 50% hardwood–50% softwood (HS). Other than the origin of the fibers, all procedures for handsheet fabrication were the same.

Figure 1a–c show high and low magnification SEM images of untreated handsheets for 100% softwood, 100% hardwood and a 50–50% hardwood/softwood mixture, respectively. The larger size of softwood fibers in comparison with hardwood fibers is confirmed by the SEM images of Fig. 1a–c. In addition, it was confirmed by SEM images (not shown) that a thin film of PFE (~ 100 nm) deposited on unetched handsheets did not alter the roughness (either micro- or nano-scale) of the handsheet surface (H, S, HS). This PFE deposition without oxygen etching yielded “sticky” superhydrophobic properties for all three handsheets with the following advancing and receding CAs: H (CA_{adv}/CA_{rec}) — $154.3^\circ \pm 1.9^\circ / 12.5^\circ \pm 5^\circ$, S (CA_{adv}/CA_{rec}) — $149^\circ \pm 2.5^\circ / 8.5^\circ \pm 5^\circ$ and HS (CA_{adv}/CA_{rec}) — $159.4^\circ \pm 7.7^\circ / 9.65^\circ \pm 5.8^\circ$. The fact that the advancing and receding CAs are similar for all three handsheets confirms that the differences in micro- and nano-scale roughnesses due to variations in fiber types do not significantly affect the “sticky” superhydrophobic behavior.

In subsequent experiments, handsheets were etched in an oxygen plasma for different durations before depositing the PFE film. Figure 2 displays plots of advancing and receding CAs for the different handsheets as a function of oxygen etching time. The figure shows the transition from “sticky” to “roll-off” superhydrophobicity (contact angle hysteresis $< 10^\circ$) after ~ 30 minutes of etching for all substrates. The curves in Fig. 2 overlap, showing that the rate of change of advancing and receding CAs, which is closely connected to the evolution of nano-scale features, was indistinguishable for the three handsheets within experimental error. Indeed, there were no noticeable differences between the sizes of the nano-scale features formed on etched hardwood and softwood fibers (SEM images not shown). These results provide evidence that there is no significant difference between the nano-scale features formed on fibers of different types. In conclusion, different fiber type does not affect the superhydrophobic behavior provided that the paper making procedures are constant.

3.1.2. Effects of Paper Making

The pulping process and the paper machine configuration vary from mill to mill in order to optimize paper properties for specific applications [25]. The process involves the following steps: after wood chips are pulped and bleached, the paper web is formed in the paper machine, after which it undergoes a variety of mechanical treatments (pressing, drying and calendering) before being collected on a large roll [27]. All these steps of the paper making process ultimately affect the roughness of the final paper surface. Each paper mill uses a unique set of paper making procedures and sequences depending on the application of the final paper product. Our

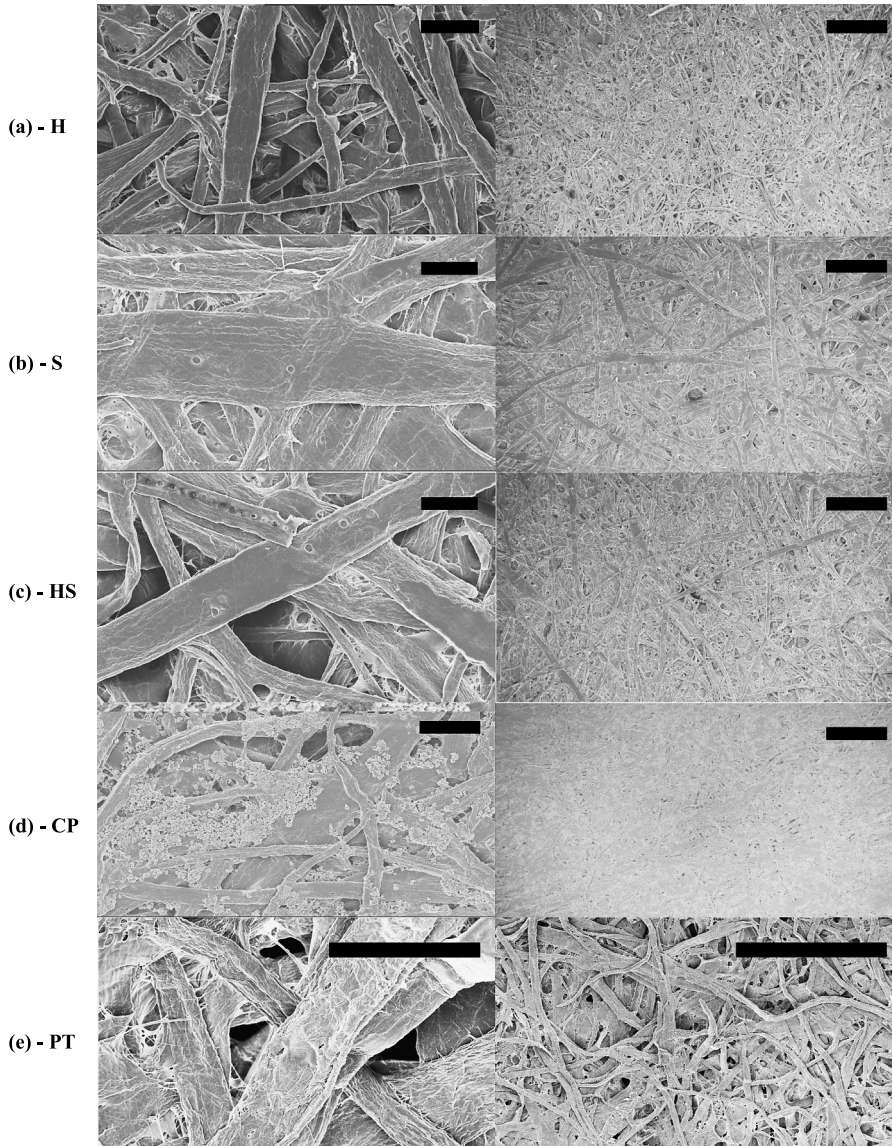


Figure 1. High (left) and low (right) magnification SEM images of laboratory handsheets made with (a) 100% hardwood (H), (b) 100% softwood (S), (c) 50–50% hardwood and softwood (HS), and two commercial paper samples, (d) copy paper (CP) and (e) paper towel (PT). Scale bars correspond to 40 μm (high magnification) and 400 μm (low magnification).

focus in this study does not involve a comprehensive investigation of the large number of parameters invoked in paper making and their effect on superhydrophobicity. Rather, we have selected two different paper types (apart from the laboratory-made handsheets) that were fabricated for unique and distinct applications: (1) a commercial copy paper (CP) which is moderately hydrophobic to yield good printability

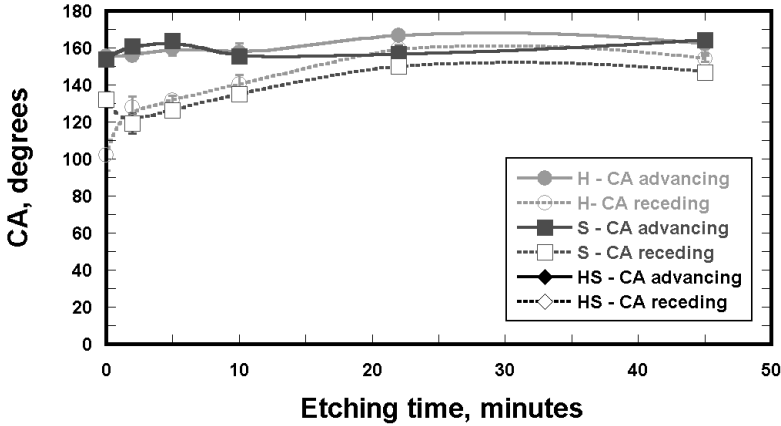


Figure 2. Plots of advancing CA and receding CA of handsheets (H, S, HS) with respect to oxygen plasma etching time for 2 min PFE deposition (~ 100 nm).

and (2) a paper towel (PT) which is extremely hydrophilic to provide high absorptivity. The copy paper and paper towel also represent two extremes of porosity and hence micro-scale roughness. Finally, the copy paper contains a significant amount of filler particles which are of similar size to the nano-scale features formed during oxygen plasma etching. Our intent in this part of the work is to explore the superhydrophobic properties of copy paper and paper towels in order to obtain insight into the effect of paper-making parameters on superhydrophobicity.

The SEM images in Fig. 1d and e show high and low magnification SEM images of untreated CP and PT, respectively. Of these two samples, the copy paper is most similar to the handsheets; the main difference is the presence of (inorganic) filler particles on the fiber surface (shown in Fig. 1d). The paper towels have a noticeably more porous surface with very loosely cross-linked fibers, since these substrates are designed for superior absorption properties. From the SEM images it is evident that these substrates have very different surface roughness values prior to plasma treatment.

The untreated copy paper displayed an advancing $CA \sim 79.15^\circ \pm 3.37^\circ$, which confirmed its moderately hydrophobic behavior. For the untreated paper towel, the water drop was absorbed into the paper within one second; therefore CA values could not be measured. After deposition of a thin film of PFE (without oxygen etching), the CP and PT substrates yielded different superhydrophobic behavior than that of the HS substrate as shown in Fig. 3. The difference in receding CA values between the samples can be attributed to differences in the micro- and nano-scale roughness that result from the distinct processing conditions in the paper mills (evident from the SEM images in Fig. 1). The advancing and receding CA values for CP, which is most similar to the HS handsheet with regard to fiber composition, are analogous to the values obtained for HS. However, the PT showed a very different receding CA relative to those for HS and CP. The increased values of the

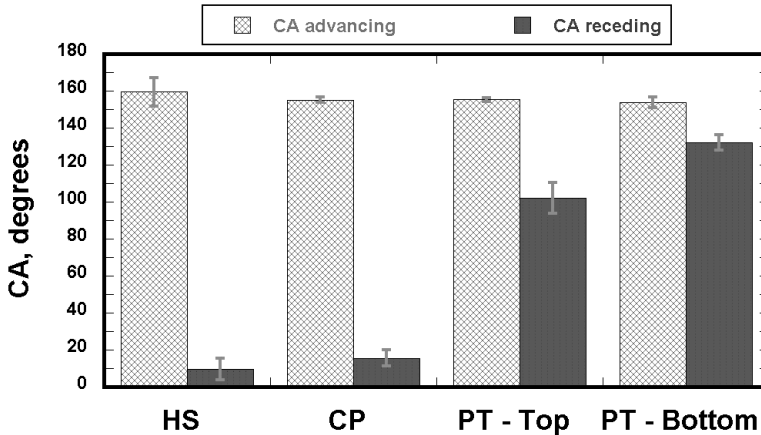


Figure 3. Plots of advancing and receding CAs of handsheet (HS), copy paper (CP), paper towel-top side (PT-top) and paper towel-bottom side (PT-bottom), after 2 min PFE deposition (~ 100 nm) and without oxygen etching.

receding CA (decreased CA hysteresis) of the PT can be attributed to the increased micro-scale roughness resulting from the increased porosity of this substrate. In addition, the PT showed different superhydrophobic behaviors on the two sides of the substrate (labeled PT-top and PT-bottom in Fig. 3). Although the SEM images did not reveal a significant difference between the two sides, we believe that the distinct CA values are due to the different roughness scales generated on the felt side and wire side of the paper during the manufacturing process, usually referred to as “two sidedness of paper” [10, 25]. The copy paper did not show a difference in superhydrophobic behavior between the top and bottom sides, which is expected since the applications of copy paper require that it has the same physical and chemical properties on both sides.

The paper substrates (CP, PT-top and PT-bottom) were subsequently etched in an oxygen plasma environment for different durations prior to PFE deposition. The advancing and receding CAs of these substrates with respect to oxygen etching times are shown in Fig. 4. It is evident from Fig. 4 that “roll-off” superhydrophobic behavior could be obtained for all samples tested, in spite of significant differences in paper making methods. Indeed, the nano-scale roughness established by oxygen etching, which is responsible for the “roll-off” superhydrophobic behavior, was similar for all papers (SEM images not shown).

In conclusion, the difference in CA hysteresis between various paper samples (Fig. 3) results in differences in the adhesion of water drops on these substrates. This demonstrates that by control of the paper making processes, adhesion of water drops on a superhydrophobic paper surface can be tuned. Also, after the paper substrates are etched, the formation of nano-scale roughness dominates the superhydrophobic behavior, thereby leading to more similar wettability for all tested paper substrates. Although these experiments do not represent a comprehensive study of the array

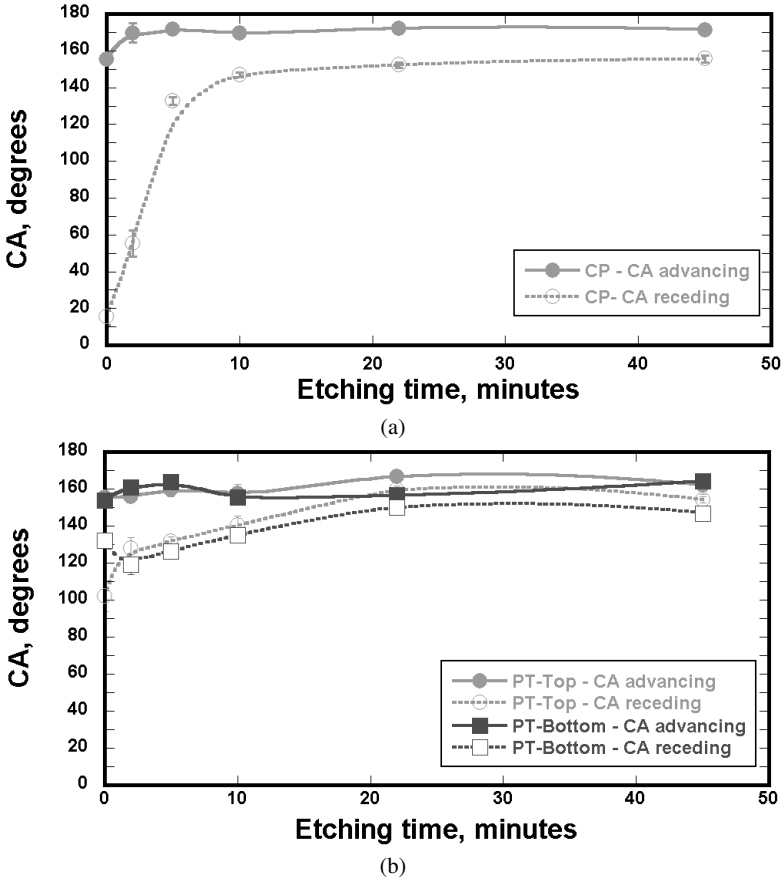


Figure 4. Plots of advancing CA and receding CA of copy paper (CP) (a) and paper towel (PT-top and PT-bottom) (b) with respect to oxygen plasma etching time for 2 min PFE deposition.

of paper making parameters, they do provide a general picture of the effects of these parameters on superhydrophobicity as established by our plasma treatment process. Furthermore, we conclude that, provided the fibers can be etched to create nano-scale features, superhydrophobicity can be imparted on any paper surface irrespective of the fiber origin or paper making technique.

3.2. Design of Superhydrophobic Paper Surfaces by Optimizing Fiber Type and Plasma Processing Conditions

Longer softwood fibers are usually responsible for paper strength, while shorter hardwood fibers are predominantly responsible for the paper shininess because of reduced roughness. Our experiments indicated that oxygen etching ultimately reduces the shininess of the paper by creating nano-scale roughness, so that the presence of hardwood fibers no longer provides enhanced optical properties in the etched handsheets. Therefore, we believe that the fabrication of superhydrophobic

paper based on softwood fibers is the most desirable approach because of the expected increased physical strength.

For longer PFE deposition times than are shown in the preceding figures (e.g., 15 minutes), roll-off superhydrophobic behavior can only be achieved after 60 minutes etching (data not shown), while for 2 min PFE deposition times roll-off is observed after much shorter etching times (~ 30 minutes) [22]. These results are due to smoothing of the topography of the roughened surface that occurs during the deposition of a thicker PFE film. Since prolonged oxygen etching damages the fiber surfaces, it has a significant negative impact on the strength of the paper, which is undesirable. Therefore, it is most desirable to obtain roll-off superhydrophobicity at reduced etch times. We expect that an optimum PFE thickness exists: thick enough to retard the absorption of water, yet thin enough to prevent smoothing of the morphology created by oxygen etching. Our results suggest that a ~ 100 nm film obtained from a 2 min PFE deposition is a near-optimum thickness to achieve a roll-off superhydrophobic paper surface with good physical properties. Of course, optimizing the paper making process to tune the micro-scale roughness may offer an additional degree of freedom for the design of superhydrophobic paper surfaces.

3.3. Effect of Drop Size on Contact Angle and Edge Geometry

Measurement of contact angles on rough surfaces is more complex when the drop size is comparable to the roughness length scale of the substrate. Advances in drop dispense technologies have made it possible to vary the dispensed volume of a water drop in a controlled manner from a few picoliters to a few microliters. Here we present results that describe the significance of the water drop size when measuring CAs on paper surfaces.

Figure 5 shows the contact line established by water drops of four different volumes on a HS handsheet with CA characteristics shown in Fig. 3. Solid lines were drawn along the three-phase contact lines to highlight the contact line geometry. Clearly, the contact line is more distorted by the topography of the fiber network for smaller drops (Fig. 5a and b) than for larger drops (Fig. 5c and d).

In order to determine the effect of contact line distortion on the measurement of CA, we varied the drop volume from $0.1 \mu\text{l}$ to $16 \mu\text{l}$, and measured the advancing CA values. Figure 6 shows the advancing CA with respect to drop volume for HS substrates etched for three different etching durations. Figure 7 shows the images of water drops corresponding to a 30 min etched HS (“roll-off” superhydrophobic) and 0 min etched HS (“sticky” superhydrophobic). From Fig. 6 it can be concluded that the advancing CA increases up to a volume of $\sim 2 \mu\text{l}$. This suggests a lower limit of drop volume that should be used to measure CA on superhydrophobic paper surfaces. On the other hand, the upper limit depends on the angular resolution of the CA goniometer. As the drop volume increases, the drop flattens due to gravity, which makes it difficult to locate exactly the three-phase contact point from a side view of the drop. This limitation can greatly affect the accuracy of CA values, which is consistent with the observation of a slight decrease in the advancing CA values for

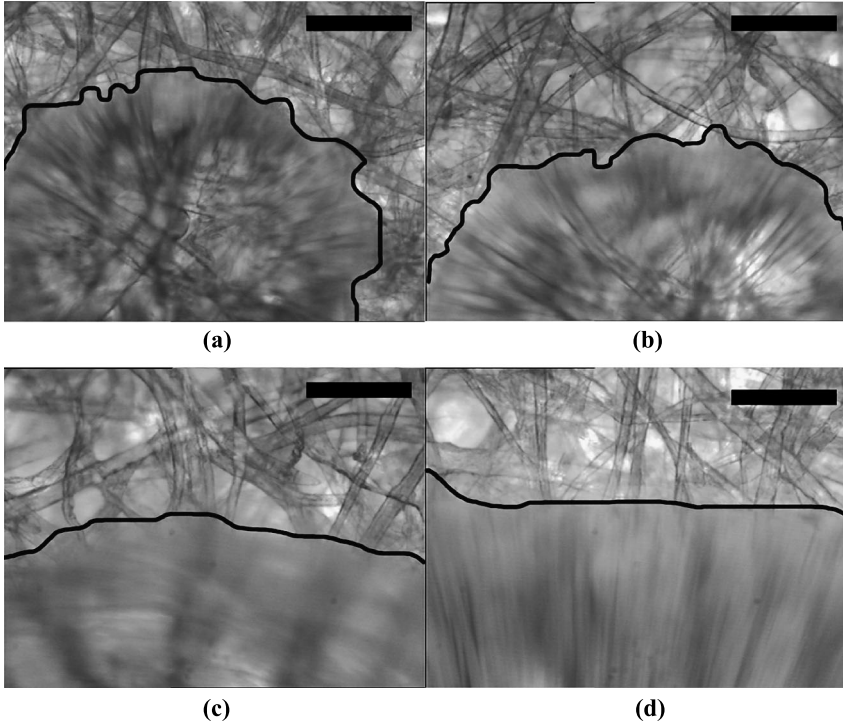


Figure 5. Contact lines formed by 0.1 μl (a), 0.2 μl (b), 4 μl (c) and 8 μl (d) water drops on a 2 min PFE deposited (without etching) HS substrate. Scale bars correspond to 160 μm .

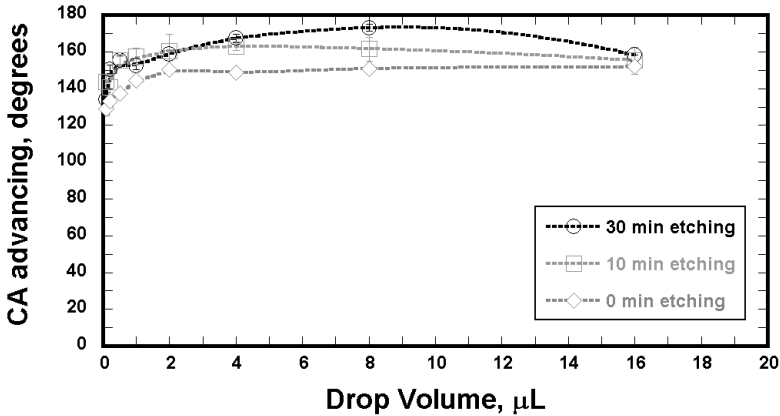


Figure 6. Plots of advancing CA with respect to drop volume for oxygen etched (0, 10 and 30 min) and PFE deposited (2 min) handsheet (HS) surfaces.

the 16 μl drop (Fig. 6). Hence, we suggest that in order to mitigate ambiguity in CA values when measuring contact angles on porous, heterogeneous substrates such as paper, it is important to select drop sizes that (1) are larger than the length scale

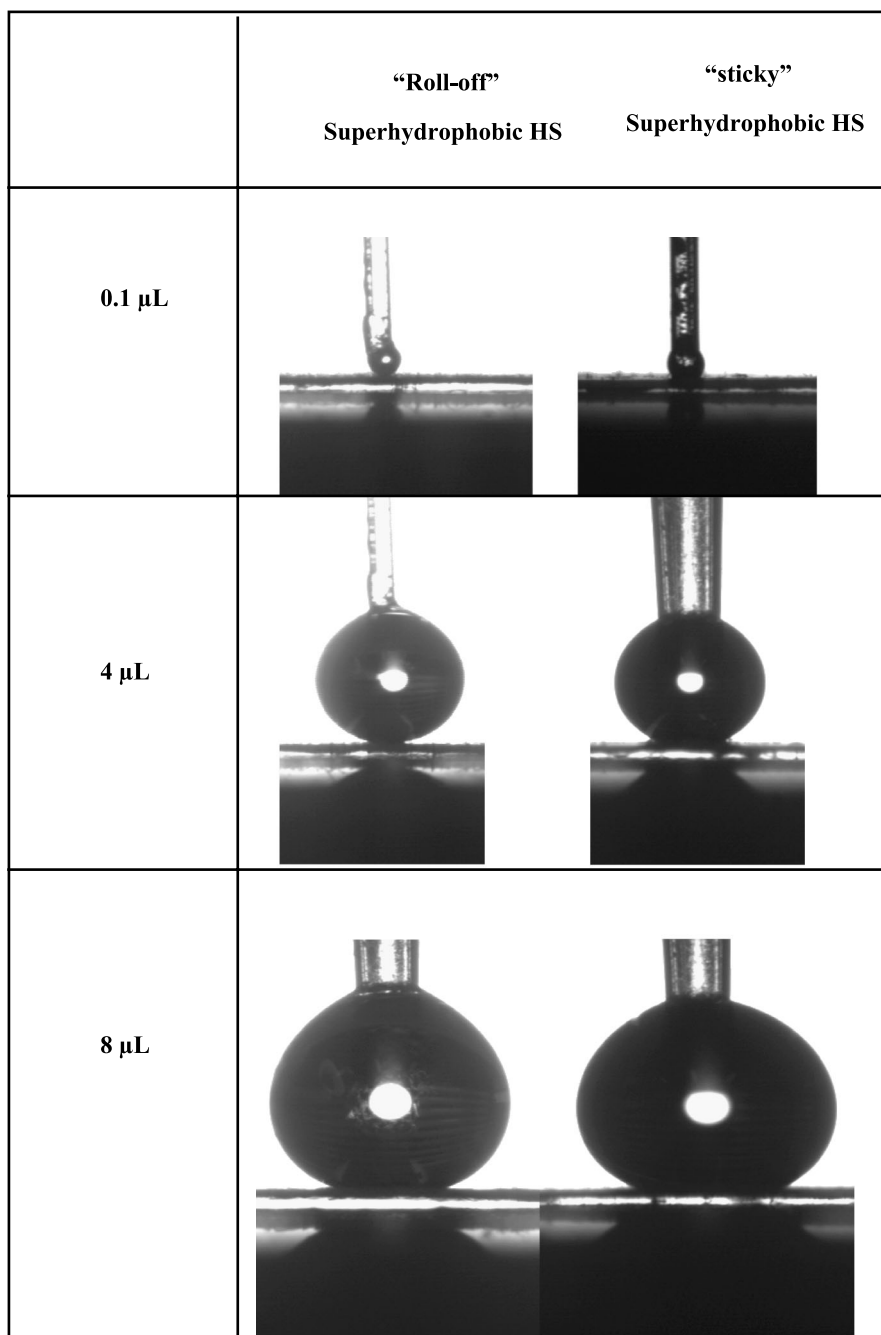


Figure 7. Photographs of advancing CA for different drop volumes for “roll-off” superhydrophobic (0 min oxygen etched and 2 min PFE deposited) and “sticky” superhydrophobic (30 min oxygen etched and 2 min PFE deposited) handsheet (HS) surfaces.

of fibers (to avoid the distortion of the contact line by fiber web) and (2) provide sufficient image resolution for the goniometer to identify the three-phase contact line.

4. Conclusions

The effects of fiber type and paper making parameters on the creation of superhydrophobic paper surfaces were studied. The different fiber types and the paper making techniques do not affect the superhydrophobicity provided that the fibers can be etched to create the necessary nano-scale surface features. Paper made from softwood fibers is likely to be more suitable for superhydrophobic applications because of improved physical properties with this fiber type, in particular paper strength. A PFE film of ~ 100 nm represents a near-optimum thickness to obtain superhydrophobicity. The importance of water drop volume in the measurement of CAs on superhydrophobic surfaces fabricated on heterogeneous and porous substrates such as paper has been discussed.

Acknowledgements

The authors thank Dr. Ashwini Sinha (Praxair) for kindly donating the PFE gas, Yonghao Xiu (Georgia Tech) for support with CA measurements. B. B. thanks the Institute of Paper Science and Technology (IPST) at Georgia Tech for fellowship support.

References

1. N. Yang and Y. L. Deng, *J. Appl. Polym. Sci.* **77**, 2067–2073 (2000).
2. Y. Ishida, H. Ohtani, S. Tsuge and T. Yano, *Anal. Chem.* **66**, 1444–1447 (1994).
3. F. Wang and H. Tanaka, *J. Appl. Polym. Sci.* **78**, 1805–1810 (2000).
4. K. Asakura, M. Iwamoto and A. Isogai, *J. Wood Chem. Technol.* **25**, 13–26 (2005).
5. M. J. Lindstrom and R. M. Savolainen, *J. Dispersion Sci. Technol.* **17**, 281–306 (1996).
6. T. Yano, H. Ohtani, S. Tsuge and T. Obokata, *Analyst* **117**, 849–852 (1992).
7. S. M. Mukhopadhyay, P. Joshi, S. Datta, J. G. Zhao and P. France, *J. Phys. D — Appl. Phys.* **35**, 1927–1933 (2002).
8. S. Vaswani, J. Koskinen and D. W. Hess, *Surf. Coat. Technol.* **195**, 121–129 (2005).
9. A. G. Cunha, C. S. R. Freire, A. J. D. Silvestre, C. P. Neto, A. Gandini, E. Orblin and P. Fardim, *Biomacromolecules* **8**, 1347–1352 (2007).
10. H. T. Sahin, S. Manolache, R. A. Young and F. Denes, *Cellulose* **9**, 171–181 (2002).
11. B. Balu, V. Breedveld and D. W. Hess, *Langmuir* **24**, 4785–4790 (2008).
12. H. Yang and Y. Deng, *J. Colloid Interface Sci.* **325**, 588–593 (2008).
13. D. Nystrom, J. Lindqvist, E. Ostmark, A. Hult and E. Malmstrom, *Chem. Commun.*, 3594–3596 (2006).
14. S. H. Li, S. B. Zhang and X. H. Wang, *Langmuir* **24**, 5585–5590 (2008).
15. Y. Yao, X. Dong, S. Hong, H. Ge and C. C. Han, *Macromol. Rapid Commun.* **27**, 1627–1631 (2006).

16. A. Winkleman, G. Gotesman, A. Yoffe and R. Naaman, *Nano Lett.* **8**, 1241–1245 (2008).
17. D. Quere, M. J. Azzopardi and L. Delattre, *Langmuir* **14**, 2213–2216 (1998).
18. K. S. Liao, A. Wan, J. D. Batteas and D. E. Bergbreiter, *Langmuir* **24**, 4245–4253 (2008).
19. Y. B. Li, M. J. Zheng, L. Ma, M. Zhong and W. Z. Shen, *Inorg. Chem.* **47**, 3140–3143 (2008).
20. R. Di Mundo, F. Palumbo and R. d'Agostino, *Langmuir* **24**, 5044–5051 (2008).
21. S. Boduroglu, M. Cetinkaya, W. J. Dressick, A. Singh and M. C. Demirel, *Langmuir* **23**, 11391–11395 (2007).
22. B. Balu, J. S. Kim, V. Breedveld and D. W. Hess, *J. Adhesion Sci. Technol.* **23**, 361–380 (2009).
23. A. M. Gaudin, A. F. Witt and T. G. Decker, *Trans. of the Society of Mining Engineers of AIME* **226**, 107–112 (1963).
24. A. M. Schwartz and F. W. Minor, *J. Colloid Sci.* **14**, 584–597 (1959).
25. H. Goyal, <http://www.paperonweb.com> (2007).
26. G. Fewless, <http://www.uwgb.edu/BIODIVERSITY> (2006).
27. A. W. C. Company, <http://www.chesterton.com/industries/process.asp?industry=24&process=51> (2008).